Journal of Inflammation Research

Dovepress
Taylor & Francis Group

Open Access Full Text Article

ORIGINAL RESEARCH

Identification and Validation of ALOX15 as a Robust Diagnostic Biomarker for Obesity-Associated Asthma: An Integrative Bioinformatic and Experimental Study

Hongsen Zhang[1–3], Linjie Chen[1–3], Haojie Chen[1–3], Kunyi Zhang[1–3], Zinan Chen[1–3], Tongsheng Chen[1,2,4]

[1]Key Laboratory of Functional and Clinical Translational Medicine (Fujian Province University), Xiamen Medical College, Xiamen, Fujian, 361023, People's Republic of China; [2]Institute of Respiratory Diseases, Xiamen Medical College, Xiamen, Fujian, 361023, People's Republic of China; [3]Department of Clinical Medicine, Xiamen Medical College, Xiamen, Fujian, 361023, People's Republic of China; [4]Department of Physiology, School of Basic Medical Sciences, Xiamen Medical College, Xiamen, Fujian, 361023, People's Republic of China

Correspondence: Tongsheng Chen, Email chentongsheng@xmmc.edu.cn

Background: Obesity is a significant independent risk factor for asthma severity. However, the underlying molecular mechanisms by which it exacerbates asthma development remain unclear. This study aims to identify and validate key hub genes involved in high-fat diet-induced obesity aggravating asthma.

Methods: Candidate genes associated with asthma, obesity, immunity, and inflammation were identified by integrating GEO databases (GSE76262, GSE41863, and GSE65204) with the GeneCards database. These candidate genes were further screened using three machine learning algorithms (LASSO, Random Forest, and SVM-RFE) followed by SHAP analysis. The expression of the hub gene ALOX15 and its correlation with pulmonary pathological changes were validated in a high-fat diet-induced asthma mouse model using qRT-PCR, Western Blot, and histological staining. Immune cell infiltration and functional pathways were explored using CIBERSORT, GSEA, and GSVA technologies.

Results: Among 233 asthma differentially expressed genes, nine candidate genes associated with obesity, immunity, and inflammation were identified. Machine learning further identified ALOX15, IL1R1, TNFAIP3, and NLRP3 as diagnostic candidate genes, with ALOX15 demonstrating the most robust performance across multiple datasets (AUC > 0.7) and confirmed as the primary predictor via SHAP analysis. Animal experiments confirmed that a high-fat diet significantly exacerbated pulmonary inflammation and airway remodeling. ALOX15 expression in lung tissue was markedly higher in high-fat diet asthma model mice compared to normal diet asthma model mice. Functional analysis revealed a positive correlation between ALOX15 and eosinophil infiltration, with significant enrichment in arachidonic acid metabolism, NF-κB signaling pathways, and lipid metabolism processes.

Conclusion: ALOX15 is a key molecular bridge in the pathogenesis of obesity-exacerbated asthma, linking high-fat diet-induced metabolic dysfunction to pro-inflammatory immune responses in the lungs, and may serve as a potential diagnostic biomarker and therapeutic target for obesity-associated asthma.

Keywords: ALOX15, obesity-associated asthma, high-fat diet, machine learning, eosinophilic inflammation

Introduction

Asthma is a heterogeneous chronic inflammatory airway disease that has become a major global health challenge.[1] At the same time, the escalating global prevalence of obesity has emerged as an important independent risk factor for the onset and severity of asthma.[2] Mendelian randomization studies have suggested a causal association between visceral obesity and elevated asthma risk.[3] Clinical evidence suggests that obesity is associated with increased prevalence of asthma, increased frequency of exacerbations, and decreased response to treatment, defining a distinct "obesity-associated

https://doi.org/10.2147/JIR.S603984
Received: 23 February 2026
Accepted: 29 April 2026
Published: 12 May 2026

asthma" phenotype.[4] While numerous inflammatory markers have been proposed to characterize this phenotype,[5–7] their diagnostic precision and clinical utility remain inconsistent. Furthermore, the intricate molecular mechanisms by which metabolic stress and lipid dysregulation exacerbate airway inflammation are not yet fully elucidated. Notably, there remains a significant gap in research that integrates comprehensive multi-cohort transcriptomic analysis with robust in vivo validation, hindering the identification of key metabolic drivers and the development of targeted interventions.

Obesity is not merely an abnormality of energy storage, but a systemic state of low-grade chronic inflammation.[8] It is characterized by immune cell activation and pro-inflammatory cytokine release, and this inflammation is thought to spread to the airways.[9] Although this broad inflammatory background has been recognized, the molecular mediators and pathways through which high-fat diet-induced metabolic stress translates into amplified and dysregulated immune responses in the asthmatic lungs remain unclear. Thus, the discovery of these key drivers is critical to move from epidemiologic observations to mechanistic understanding, which can help advance precision diagnosis and treatment for this complex asthma subtype.

Many studies[10–12] have shown that the dynamic crosstalk between dysregulated lipid metabolism and immune cell function is a central mechanism of obesity-exacerbated asthma. Bioactive lipid mediators, including eicosanoids derived from polyunsaturated fatty acids, are potent regulators of bronchoconstriction, inflammation, and immune cell recruitment.[13] Among the enzymes regulating eicosanoids biosynthesis, lipoxygenases (LOXs) are of particular interest. Arachidonic acid 15 - lipoxygenase (ALOX15) catalyzes the oxidation of arachidonic acid, and its metabolites play an important role in inflammation and its resolution.[14] Although ALOX15 is known to be involved in classical allergic asthma primarily through eosinophil activation,[15] its specific role as a central integrator of high-fat dietary signals, lipid metabolic remodeling, and exacerbated immune responses in obesity-associated asthma is unknown.

This study integrates data from the Gene Expression Omnibus (GEO) and GeneCards databases to identify key intersecting genes. Three machine learning algorithms were used to screen for robust diagnostic biomarkers and analyzed using SHapley Additive exPlanations (SHAP) to improve model transparency and mitigate the "black-box" nature of predictive results. The biological relevance of the identified hub genes was further validated in a high-fat diet (HFD)-induced asthma mouse model. Specifically, our study provides a unique contribution by identifying ALOX15 as a pivotal molecular bridge between high-fat diet-induced metabolic dysfunction and allergic airway inflammation. By elucidating this mechanism, we offer a novel therapeutic target specifically tailored for the refractory "obese-asthma" phenotype, which often exhibits poor responsiveness to conventional treatments. The aim of this study is to elucidate the crosstalk between obesity and asthma, and to identify new therapeutic targets and diagnostic strategies to improve the clinical outcomes of patients with refractory asthma.

Method

Data Collection

The Gene Expression Omnibus (GEO) database was searched using the keyword "asthma". Datasets with a sample size of approximately 60 or more and with both healthy controls and asthma patients were selected for analysis. Three eligible datasets (GSE76262, GSE41863, and GSE65204) were subsequently included for analysis. GSE76262 was used as the training set, and GSE41863 and GSE65204 were used as the validation set. In the training set (GSE76262), 21 healthy samples were utilized as the Control group and 93 severe asthma samples constituted the Asthma group. For the validation sets, samples were similarly categorized into Control and Asthma groups for GSE41863 (n = 9 and n = 47, respectively) and GSE65204 (n = 33 and n = 36, respectively).

Animal Models and Experimental Design

Animal procedures were conducted in accordance with the Guide for the Care and Use of Laboratory Animals (8th edition, 2011, National Institutes of Health, USA) and approved by the Animal Care and Use Committee of Xiamen Medical College (Approval No. 20250804026). Thirty female BALB/c mice (6 weeks old, 12–14 g) were randomly assigned to four groups (n = 7–8/group): Control (Ctrl), Normal Diet Asthma (NDA), High-Fat Diet (HFD), and High-

Fat Diet Asthma (HFDA). Mice were maintained under standard laboratory conditions with 12-h light/dark cycle and *ad libitum* access to food and water.

The Ctrl and NDA groups received a normal diet (ND), whereas the HFD and HFDA groups were fed a high-fat diet (HFD). Body weights were recorded every three days. After a four-week dietary period, asthma was induced in the NDA and HFDA groups. Briefly, mice were sensitized via intraperitoneal injections of an OVA suspension (100 μg OVA and 2 mg aluminum hydroxide in 0.2 mL saline) on days 0, 7, and 14. Non-asthmatic groups (Ctrl and HFD) received sham injections of saline and aluminum hydroxide. From days 21 to 26, the NDA and HFDA groups were challenged with aerosolized 1% OVA (10 mg/mL) at a flow rate of 0.5 mL/min for 30 minutes daily to induce airway inflammation. Control mice were nebulized with saline according to the same protocol. After the final challenge, all mice were euthanized by cervical dislocation, and lung tissue was collected for subsequent analysis.

Histological Analysis

Mouse lung tissues were fixed in 4% paraformaldehyde for 24 h, dehydrated through a graded ethanol series, and embedded in paraffin. Sections (4–5 μm thick) were then subjected to Hematoxylin and Eosin (H&E) staining. Pathological alterations, including inflammatory infiltration, goblet cell hyperplasia, and collagen deposition, were evaluated via light microscopy.

Identification of Differentially Expressed Genes (DEGs)

Differential expression analysis of GSE76262 was performed using the limma package. DEGs were identified based on the screening criteria of $|\log_2$ fold change (FC)$| > 1$ and adjusted p-value < 0.05, and heatmaps and volcano plots were generated using the pheatmap and ggplot2 packages, respectively.

Identification of Candidate Genes Related to Immunity, Obesity, and Inflammation

Initially, genes associated with immunity, inflammation, and obesity were retrieved from the GeneCards database (https://www.genecards.org/). To ensure high-confidence associations, a relevance score threshold of > 3 was applied, yielding 1194 obesity-related, 1666 immunity-related, and 1,056 inflammation-related genes.

To identify key therapeutic targets, Venn diagrams were constructed using a bioinformatics online platform (https://www.bioinformatics.com.cn/) to determine the intersection between these three gene sets and the previously identified DEGs. The resulting overlapping genes were designated as candidate genes and prioritized for subsequent analysis.

Functional Enrichment Analysis

To further elucidate the biological significance of the identified candidate genes, Gene Ontology (GO) and Kyoto Encyclopedia of Genes and Genomes (KEGG) enrichment analyses were performed using the clusterProfiler R package. The results were visualized using the enrichplot and ggplot2 packages, with an adjusted p-value < 0.05 set as the significance threshold.

Machine Learning and Artificial Neural Networks Construction

Candidate key genes were identified using three different machine learning algorithms, including Random Forest (RF), Least Absolute Shrinkage and Selection Operator (LASSO) regression, and Support Vector Machine Recursive Feature Elimination (SVM - RFE). Specifically, the "randomForest" package was used to implement the RF algorithm, the "glmnet" package to perform LASSO regression, and the "e1071" package to perform SVM-RFE. The package "VennDiagram" was used to determine and visualize the intersection of the genes identified by the three algorithms. To further validate the statistical independence of the candidate genes identified by machine learning, we performed univariate and multivariate logistic regression and generated forest plots using the "glmnet" package.

Subsequently, an artificial neural network was constructed to evaluate the diagnostic efficacy of these genes using the "neuralnet" and "NeuralNetTools" packages. The input data, derived from the candidate genes, were processed through hidden layers to produce an optimized output layer, thereby establishing a robust predictive model for asthma diagnosis.

SHapley Additive exPlanations (SHAP) Analysis

To address the inherent "black box" nature of the machine learning process, we conducted an interpretive analysis using SHAP framework based on cooperative game theory. This method is applied after model construction to quantify and visualize the specific contribution of selected genes to the predicted output. By using the kernelshap package, we provide a rigorous interpretation of feature significance, effectively identifying the most influential genes involved in obesity-asthma molecular interactions. This approach ensures that the model's predictions are not only accurate but also biologically interpretable.

Identification and Validation of Key Genes

To determine the diagnostic efficacy of each candidate, Receiver Operating Characteristic (ROC) curves were constructed, and the Area Under the Curve (AUC) was calculated using the pROC package. AUC > 0.7 defined as having strong diagnostic performance. Furthermore, differential expression patterns within the GSE76262 training set were visualized via box plots using the ggpubr package.

To ensure the robustness and reproducibility of these biomarkers, both diagnostic performance and expression consistency were further evaluated in the GSE41863 and GSE65204 independent validation sets. Only genes that strictly met the dual criteria of AUC>0.7 and showed consistent differential expression in all three datasets were recognized as final key genes.

mRNA Extraction and Quantitative Real-Time PCR (qRT-PCR)

Total RNA was extracted from mouse lung tissues using TRIzol reagent (Applygen Technologies, Beijing, China) in accordance with the manufacturer's instructions. Subsequently, complementary DNA (cDNA) was synthesized using the RevertAid First Strand cDNA Synthesis Kit (Thermo Scientific, USA) following the provided protocol. qRT-PCR was then performed using the Promega GoTaq® qPCR Master Mix (Promega, Madison, WI, USA) on a real-time PCR detection system. Relative mRNA expression was quantified via the $2^{-\Delta\Delta Ct}$ method. The specific primer sequences used in this study were as follows: *ALOX15* (F: 5′-GCTGTTTGTGAGAGTGCAGAA-3′, R: 5′-AGGGGAACGTGTACTCCGAT-3′) and *18S rRNA* (F: 5′-TTGACTCAACACGGGAAACC-3′, R: 5′-AGACAAATCGCTCCACCAAC-3′).

Western Blot

Total protein was extracted from lung tissues using RIPA lysis buffer. The extracted proteins were separated via SDS-PAGE and electrotransferred onto nitrocellulose membranes. Following blocking with 5% non-fat milk in TBST for 1 h at room temperature, the membranes were incubated with primary antibodies overnight at 4°C. After three washes with TBST, the membranes were incubated with the appropriate HRP-conjugated secondary antibody (1:8000, A9169, Sigma-Aldrich) for 1 h at room temperature. Protein bands were visualized using enhanced chemiluminescence (ECL) detection reagents (Applygen Technologies, Beijing, China), and digital images were captured using the ChemiDoc MP Imaging System (Bio-Rad, USA). Quantification was performed by densitometric analysis using ImageJ software. Primary antibodies used in this study included anti-ALOX15 antibody (1:1000, ab244205, Abcam) and anti-GAPDH antibody (1:5000, AF7021, Affinity).

Immune Infiltration Analysis

The CIBERSORT algorithm was used to quantify immune cell infiltration and estimate the relative proportions of 22 different immune cell subtypes in the lung microenvironment. Stacked bar graphs were constructed using the ggplot2 package. Box line plots were generated using the ggpubr package for comparative analysis of the 22 immune cell types in the control and asthma groups. Spearman rank correlation analysis was used to assess the association between the expression levels of identified key genes and the extent of immune cell infiltration. These correlation results were visualized using the Linket program.

Gene Set Enrichment Analysis (GSEA)

To elucidate the potential biological pathways and signaling cascades regulated by the identified key genes, GSEA was performed. For each key gene, samples in the training set were divided into high-expression and low-expression groups based on the median expression level. Functional enrichment analysis was carried out using the clusterProfiler and enrichplot packages, and the results were visualized. The significance thresholds were set at $p < 0.05$ and an absolute Normalized Enrichment Score ($|NES| > 1$.

ALOX15-Based Gene Set Variation Analysis (GSVA)

Gene Set Variation Analysis (GSVA) is a gene set analysis method that is distinct from single-gene-based gene set enrichment analysis, characterized by its unsupervised and non-parametric properties. Using the GSVA package, this approach extrapolates alterations from the gene level to the pathway level at the individual sample scale, thereby identifying the biological processes in which key genes are enriched. The resulting analytical outcomes are finally subjected to visualization.

Statistical Analysis

Statistical analyses were performed using R (version 4.4.3) and GraphPad Prism 8. Data are presented as the mean ± SEM. Statistical significance was determined via Student's *t*-test or one-way ANOVA. A p-value < 0.05 was considered statistically significant.

Result

Identification of Shared Candidate Genes for Asthma, Obesity, Inflammation and Immunity

To identify key molecular drivers at the intersection of metabolic and inflammatory pathways, we performed differential expression analysis on the GSE76262 dataset, and identified a total of 233 differentially expressed genes (DEGs). The heatmap demonstrated the top 30 up-regulated genes and 30 down-regulated genes (Figure 1A). In addition, we presented the expression of these DEGs using volcano plots (Figure 1B), highlighting significant genes such as IL18R1, IL1RL1 and ALOX15. Next, these 233 DEGs were intersected with three sets of disease-related genes (1194 obesity-related genes, 1666 immune-related genes, and 1056 inflammation-related genes) obtained from the GeneCards database. As shown in the Venn diagram (Figure 1C), nine overlapping genes (VEGFA, SPP1, NLRP3, IL1R1, TNFAIP3, CCL4, CSF1, ALOX15, SLC7A11) were finally obtained. These nine genes were identified as core candidate genes for subsequent functional validation and model construction.

Functional Enrichment Analysis Identifies Immune-Inflammatory Signaling Hubs

To elucidate the potential biological mechanisms underlying the link between high-fat diet-induced obesity and asthma pathogenesis, we performed Gene Ontology (GO) and Kyoto Encyclopedia of Genes and Genomes (KEGG) enrichment analyses on nine intersecting genes. The GO analysis (Figure 2A–C) showed that these genes are mainly involved in the biological processes of leukocyte and granulocyte migration (BP), as well as in the regulation of adaptive immune responses. Regarding cellular components (CC), significant enrichment was found in the classical inflammatory vesicle complex and in the endoplasmic reticulum lumen. Molecular Functional (MF) analyses particularly emphasized cytokine activity and cytokine receptor binding, indicating strong activation of extracellular signals. The synergy between these functional terms was further visualized by enrichment networks (Figure 2B) and cluster visualization (Figure 2C). Meanwhile, KEGG pathway analysis (Figure 2D–F) showed that the identified genes were significantly enriched in the NF-κB, MAPK and PI3K-Akt signaling pathways as well as in processes associated with cell death (eg. necroptosis and ferroptosis). These results suggest that high-fat diet-induced obesity may promote asthma by activating complex immune-inflammatory networks and programmed cell death pathways.

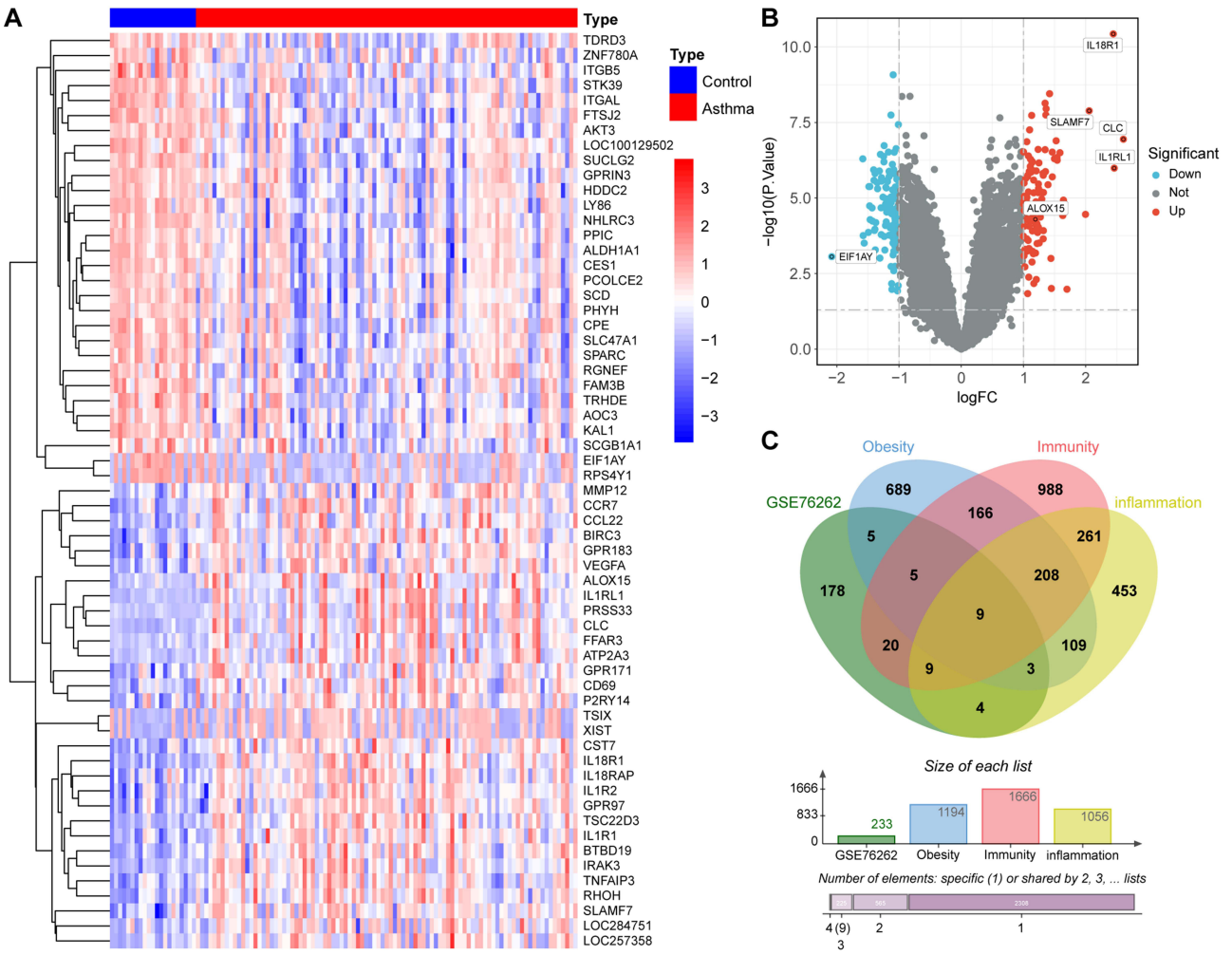

Figure 1 Identification of candidate genes. (**A**) Heatmap displaying the top 30 DEGs in GSE76262. (**B**) Volcano plot illustrating differentially expressed genes in GSE76262. (**C**) Venn diagram showing the 9 common differentially expressed genes across asthma, obesity, and immune-inflammation.

Identification of Potential Hub Genes via Machine Learning and Neural Network Modeling

To optimize the selection of the most reliable biomarkers, three machine learning algorithms were applied to further screen nine candidate genes. Six genes were identified using ten-fold cross-validated LASSO regression for feature selection (Figure 3A). The RF algorithm utilized 500 decision trees and ranked genes according to their Mean Decrease Gini scores, and nine genes with significant importance were screened (Figure 3B). In addition, the SVM - RFE algorithm used ten-fold cross-validation to evaluate the discriminative power, which resulted in the identification of eight optimal features (Figure 3C). By taking the intersection of these three methods, *ALOX15, IL1R1, TNFAIP3*, and *NLRP3* were identified as key diagnostic candidate genes (Figure 3D).

To assess the statistical independence of these genes, we performed univariate and multivariate logistic regression analyses. As shown in the forest plot (Figure 3E and F), ALOX15 exhibited excellent predictive value and was a significant independent factor in both univariate ($p < 0.001$) and multivariate ($p = 0.007$) models. Finally, an Artificial Neural Network (ANN) model consisting of four input nodes, five hidden nodes, and two output nodes was constructed using these four genes (Figure 3G). The AUC of the ROC curve was 0.986 (95% CI: 0.967–0.998, Figure 3H), indicating a reliable diagnostic performance of the ANN. These results suggest that this four-gene combination, especially ALOX15, provides a high-precision framework for the diagnosis of obesity-related asthma.

https://doi.org/10.2147/JIR.S603984

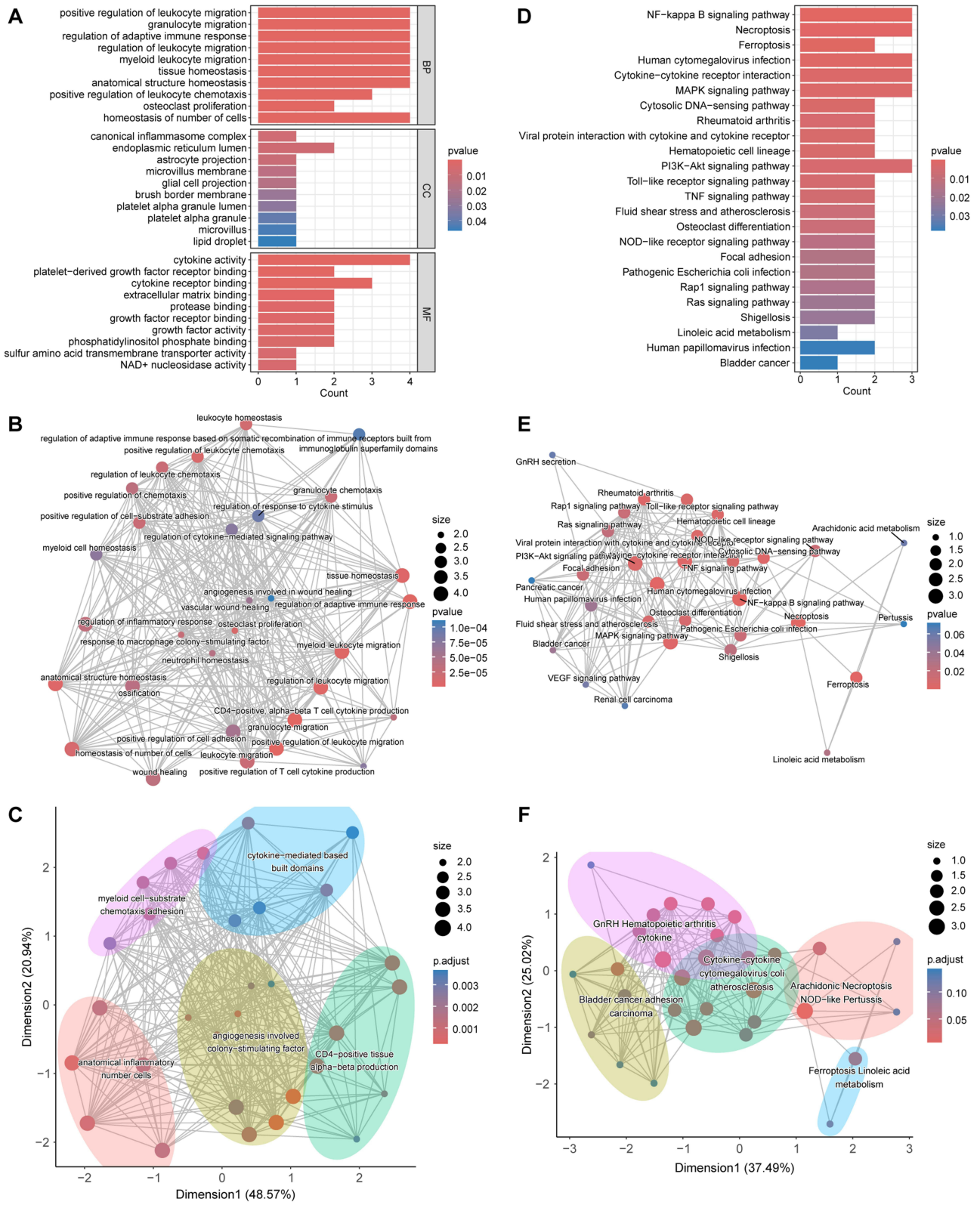

Figure 2 Functional Enrichment Analysis of the 9 Intersection Genes. (**A**) Bar plot illustrating the Gene Ontology (GO) enrichment results. (**B**) Functional enrichment network visualizing the connectivity and overlap between significant GO terms. (**C**) Clustered network of GO enrichment results. (**D**) Bar plot showcasing the enriched Kyoto Encyclopedia of Genes and Genomes (KEGG) pathways, highlighting inflammatory cascades and cell death processes. (**E**) Pathway-gene network demonstrating the crosstalk between significant KEGG pathways. (**F**) Clustered visualization of KEGG pathways, revealing the integration of signaling hubs like the NF-kappa B and PI3K-Akt pathways.

https://doi.org/10.2147/JIR.S603984

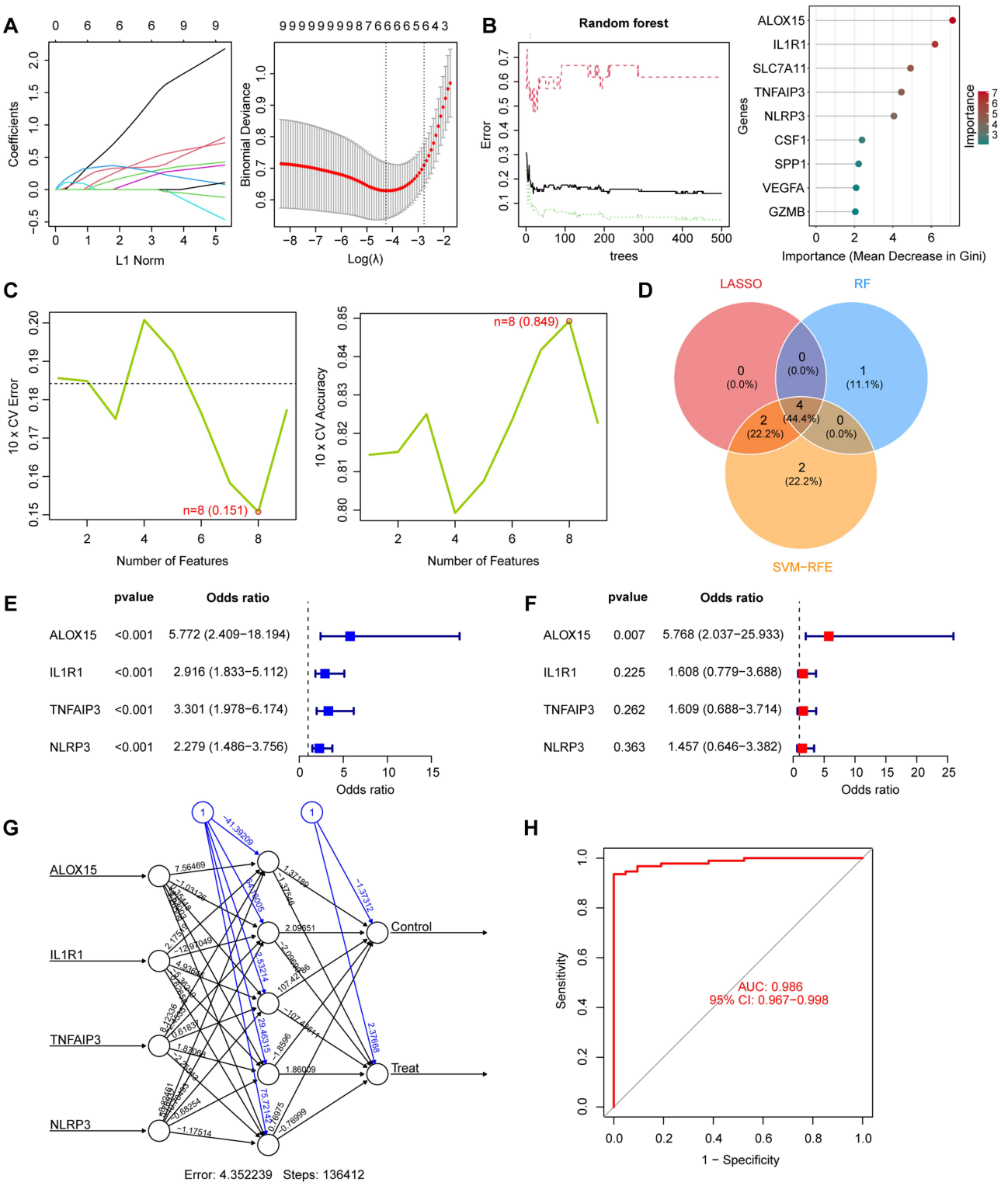

Figure 3 Identification of potential hub genes and construction of the diagnostic neural network model. (**A**) LASSO regression analysis with ten-fold cross-validation; the left panel displays the coefficient profiles of candidates, and the right panel shows the selection of the optimal λ value based on minimum binomial deviance. (**B**) Random Forest (RF) algorithm results; the left panel shows the error rate versus the number of trees, and the right panel ranks genes based on their Mean Decrease Gini scores (importance > 2). (**C**) Selection of optimal features using the Support Vector Machine-Recursive Feature Elimination (SVM-RFE) algorithm with ten-fold cross-validation; the red circles indicate the number of features with the lowest cross-validation error and highest accuracy. (**D**) Venn diagram demonstrating the intersection of genes identified by LASSO, RF, and SVM-RFE, yielding four key candidate genes. (**E-F**) Forest plots illustrating the results of (**E**) univariate and (**F**) multivariate logistic regression analyses for the four candidate genes. (**G**) Architecture of the established Artificial Neural Network (ANN) model, comprising an input layer (4 nodes), a hidden layer (5 nodes), and an output layer (2 nodes). (**H**) Receiver Operating Characteristic (ROC) curve evaluating the diagnostic performance of the ANN model in the training set (GSE76262).

https://doi.org/10.2147/JIR.S603984

Interpretability of the Machine Learning Model via SHAP Analysis

To ensure the reliability and interpretability of the diagnostic model, we first divided the dataset into a training set (70%) and an internal validation set (30%). Several machine learning algorithms were comparatively analyzed and their performance was visualized through ROC curves (Figure 4A). The Gradient Boosting Machine (GBM) was identified as the optimal algorithm, with an AUC of 0.870. In order to unveil the "black box" nature of the GBM model, we performed SHAP analysis. The SHAP importance bar plot ranked features by their mean absolute SHAP values and identified *ALOX15* as the most influential driver in the model predictions (Figure 4B). The SHAP beeswarm plot (Figure 4C) further illustrated the distribution of SHAP values, where higher expression levels of *ALOX15* and *IL1R1* were positively associated with increased probability of asthma diagnosis.

In addition, SHAP dependence plots (Figure 4D) revealed complex interactions between key genes, demonstrating how different expression levels modulate their marginal contribution to the predictive outcome. Force plots and waterfall diagrams (Figure 4E and F) were generated to provide individualized interpretations for specific samples. Collectively, the SHAP analysis provides a multi-dimensional, high-resolution interpretation of the model, further confirming that *ALOX15* is a key biomarker for obesity-related asthma.

Multi-Dataset Validation Identifies ALOX15 as a Robust Diagnostic Hub Gene

To evaluate the clinical relevance and diagnostic stability of the identified biomarkers, we performed validation using a training set (GSE76262) and two independent external validation sets (GSE41863 and GSE65204). In the training set, box plot analysis (Figure 5A) demonstrated that all four candidate genes (*ALOX15, IL1R1, TNFAIP3*, and *NLRP3*) were significantly up-regulated in asthma patients compared to healthy controls, with AUC values exceeding the threshold of 0.7 (Figure 5B). In GSE41863

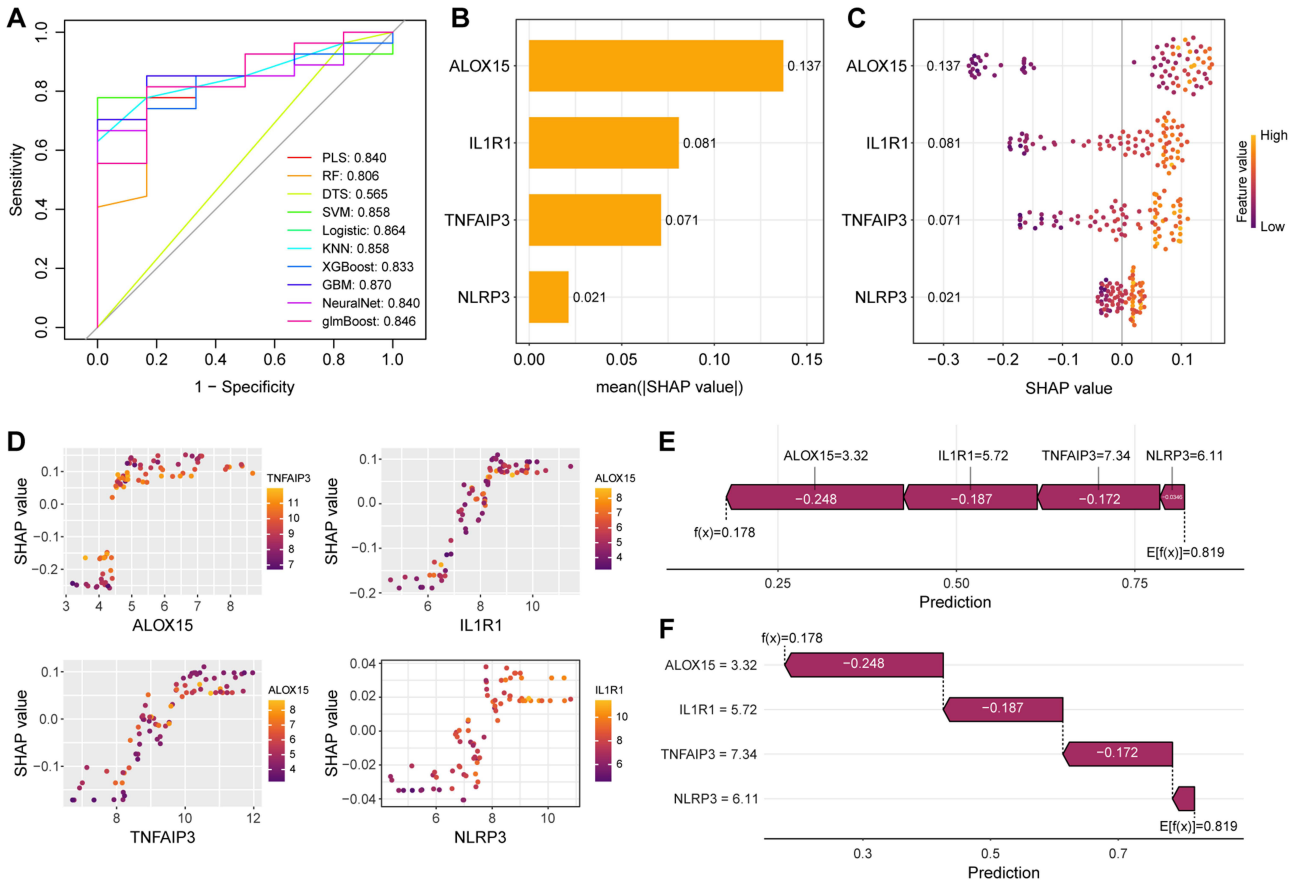

Figure 4 SHAP Interpretation of Predictive Models. (**A**) ROC analysis comparing predictive models. (**B**) SHAP importance plot ranking the four key genes based on their mean absolute SHAP values, highlighting the predominant role of *ALOX15*. (**C**) Beeswarm plot visualizing feature value-SHAP value relationships. (**D**) Dependence plot showing interaction effects between paired gene features. (**E**) Force plot illustrating feature contributions to specific predictions. (**F**) Waterfall chart demonstrating individual prediction explanations.

https://doi.org/10.2147/JIR.S603984

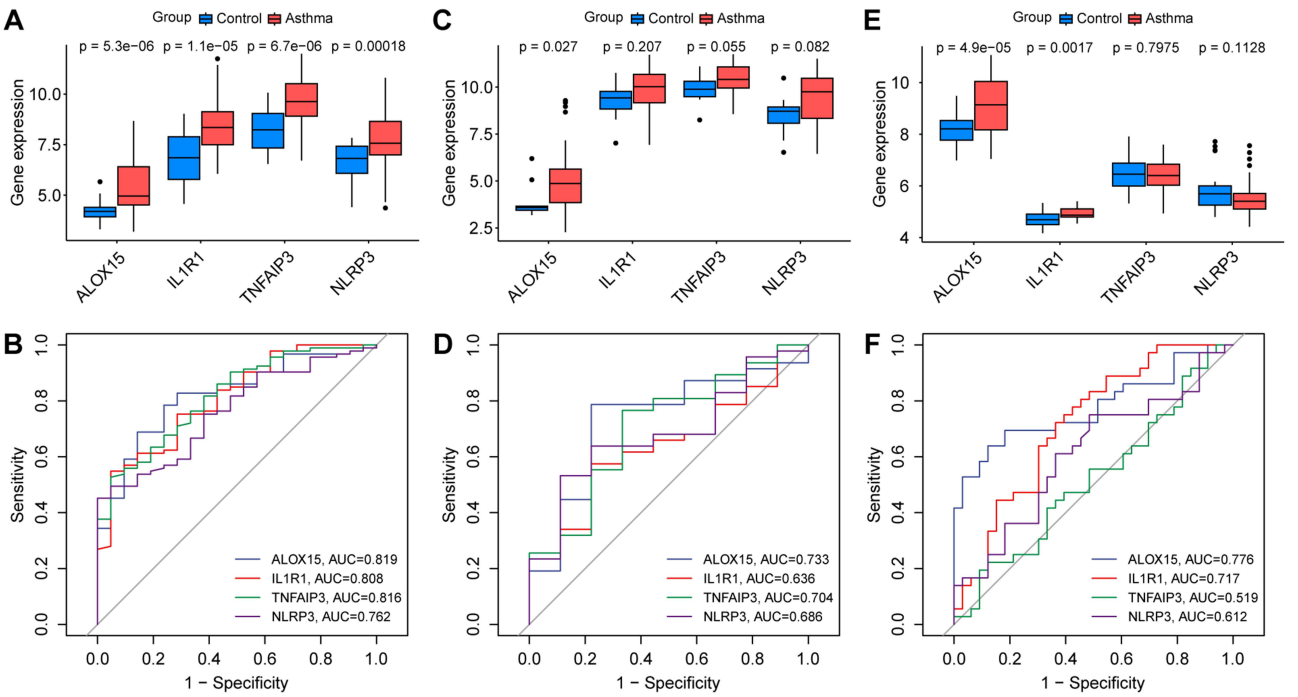

Figure 5 Validation of candidate hub genes in the training and external validation sets. (**A**) Box plots comparing the expression levels of *ALOX15, IL1R1, TNFAIP3*, and *NLRP3* between asthma patients and healthy controls in the GSE76262 training set. (**B**) Receiver Operating Characteristic (ROC) curves evaluating the diagnostic performance of the four candidate genes in GSE76262. (**C**) Box plots comparing the expression levels of *ALOX15, IL1R1, TNFAIP3*, and *NLRP3* between asthma patients and healthy controls in the GSE41863 validation set. (**D**) Receiver Operating Characteristic (ROC) curves evaluating the diagnostic performance of the four candidate genes in GSE41863. (**E**) Box plots comparing the expression levels of *ALOX15, IL1R1, TNFAIP3*, and *NLRP3* between asthma patients and healthy controls in the GSE65204 validation set. (**F**) Receiver Operating Characteristic (ROC) curves evaluating the diagnostic performance of the four candidate genes in GSE65204.

(Figure 5C and D), *ALOX15* remained significantly up-regulated in asthma patients with an AUC of 0.733, demonstrating reliable diagnostic efficacy. In GSE65204 (Figure 5E and F), *ALOX15* was similarly expressed at a significantly elevated level, with an AUC of 0.776.

Taken together, *ALOX15* consistently maintained significant differential expression and robust AUC values in all three independent datasets. Thus, *ALOX15* was identified as the key hub gene and prioritized for further investigation into its role in the immune-inflammatory mechanisms in asthma and obesity.

Experimental Validation of ALOX15 in an Obese-Asthma Mouse Model

To confirm the biological relevance of our bioinformatic findings, we established a mouse model of asthma exacerbated by a high-fat diet. HE staining (Figure 6A) showed that the lung structure was relatively intact in the normal diet (ND) and high-fat diet (HFD) groups, whereas the bronchial wall was markedly thickened, mucus secretion was increased, and there was a large perivascular inflammatory cell infiltration in the bronchial vessels in the normal diet asthma (NDA) group. These pathological features were significantly exacerbated in the HFD-induced asthma (HFDA) group, characterized by extensive inflammatory cell aggregation and narrowed airway lumens.

We then evaluated the expression of the hub gene *ALOX15* in lung tissues. qRT-PCR analysis (Figure 6B) showed that *ALOX15* mRNA levels were significantly elevated in the NDA group ($p = 0.0108$ vs. ND) and further elevated in the HFDA group ($p = 0.0002$ vs. NDA). Western blot analysis (Figure 6C and D) confirmed these results at the protein level, demonstrating that ALOX15 expression was significantly increased in HFDA mice compared to NDA mice ($p = 0.0214$). These experimental data demonstrate that ALOX15 is a key molecular driver through which a high-fat diet contributes to the pathogenesis and exacerbation of asthma.

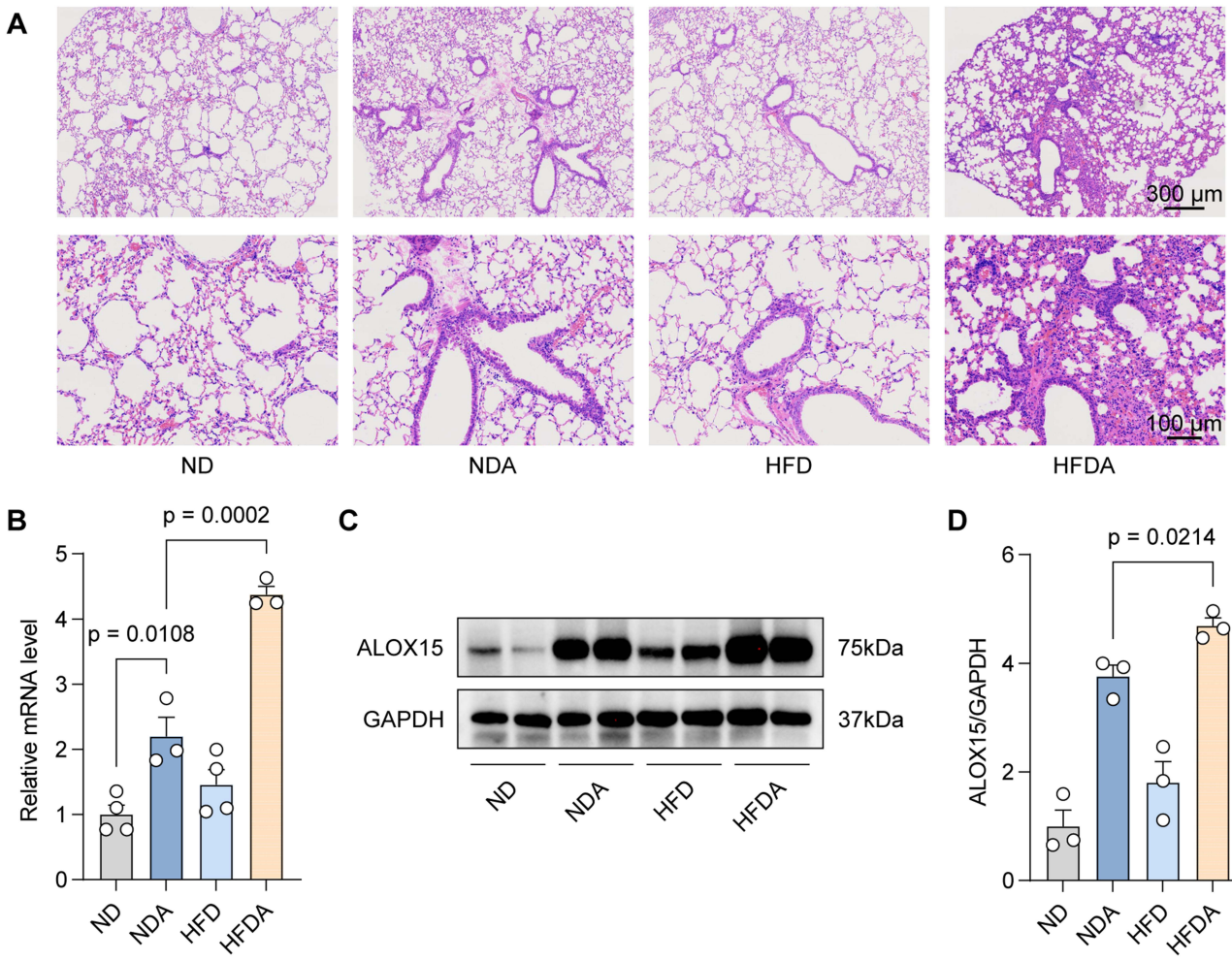

Figure 6 Experimental validation of ALOX15 expression in mouse lung tissues. (**A**) Representative Hematoxylin and Eosin (HE) stained sections of lung tissues from the ND, NDA, HFD, and HFDA groups. (**B**) Relative mRNA expression levels of ALOX15 in lung tissues determined by qRT-PCR. (**C**) Representative Western blot images showing ALOX15 protein levels across the four experimental groups; GAPDH was used as the internal loading control. (**D**) Quantitative densitometric analysis of the ALOX15/GAPDH ratio. Data are presented as the mean ± SEM (n = 3 or 4 per group). ND: Normal Diet; NDA: Normal Diet + Asthma; HFD: High-Fat Diet; HFDA: High-Fat Diet + Asthma.

Functional Analysis via GSEA and GSVA

To further elucidate the biological processes regulated by ALOX15, we performed Gene Set Enrichment Analysis (GSEA) and Gene Set Variation Analysis (GSVA). GSEA results (Figure 7A–D) indicated that the high *ALOX15* expression group was mainly enriched in glucose catabolic processes, BCL-2 family protein complexes, and the pentose phosphate pathway. In contrast, the low *ALOX15* expression group was associated with the negative regulation of viral genome replication and defense responses to symbionts. These findings suggest that *ALOX15* may shift the cellular state from anti-viral defense toward pro-inflammatory and metabolic-active phenotypes.

GSVA (Figure 7E and F) revealed that *ALOX15* was significantly enriched in lipid metabolism-related pathways, particularly linoleic acid and arachidonic acid metabolism, as well as lipoxin and hepoxilin biosynthetic processes. Notably, GSVA also highlighted significant enrichment in autophagosome assembly, chemokine receptor binding, and NF-κB signaling pathway. These results suggests that *ALOX15* acts as a central node linking lipid metabolic dysfunction with cytoplasmic ribosome activity and innate immune signaling. This multifaceted regulatory network may underlie the molecular mechanism by which a high-fat diet exacerbates inflammatory responses in asthma.

https://doi.org/10.2147/JIR.S603984

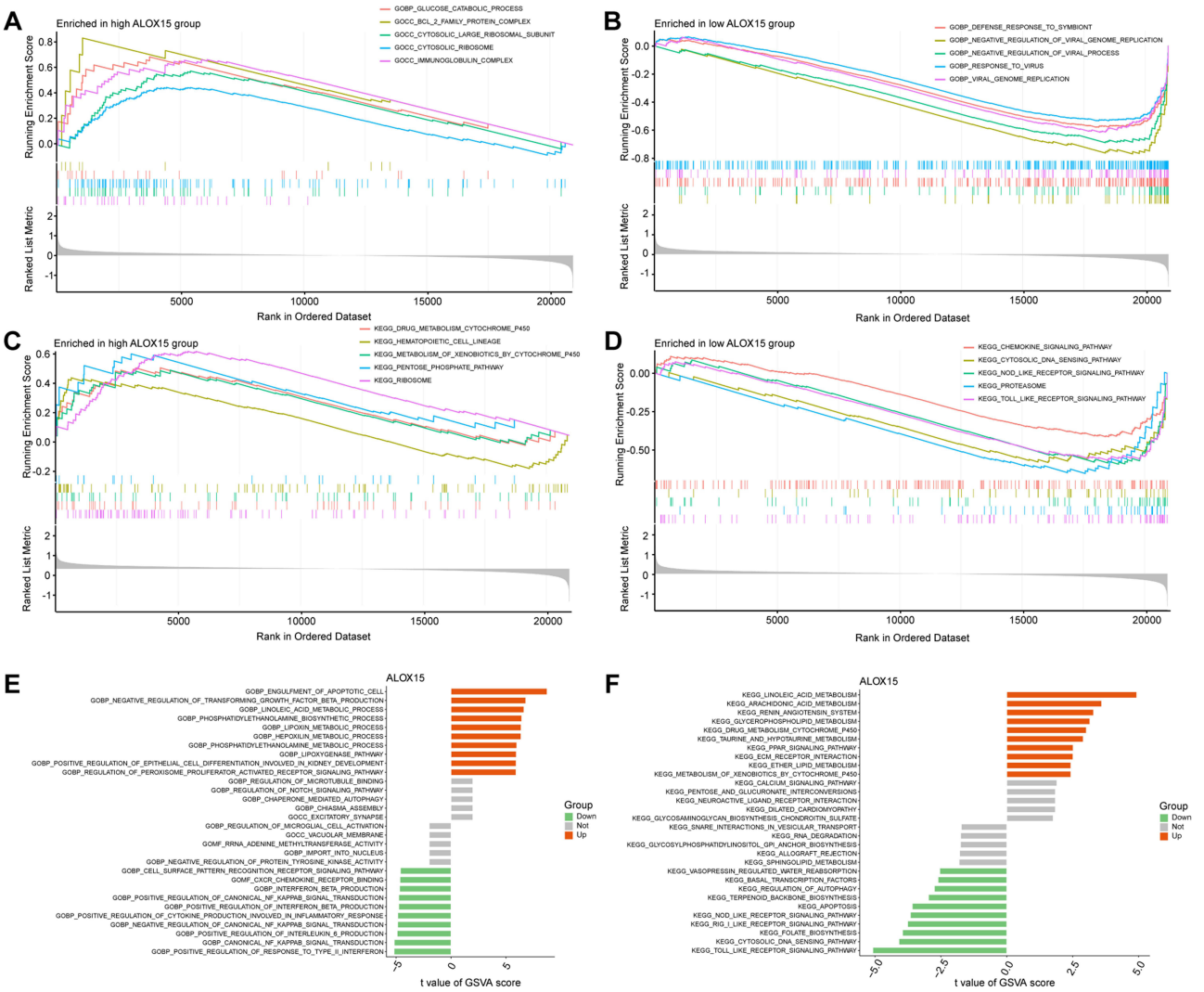

Figure 7 Functional characterization of ALOX15 via GSEA and GSVA. (**A** and **B**) GSEA results showing significant GO terms enriched in the (**A**) high ALOX15 expression group and (**B**) low ALOX15 expression group. (**C** and **D**) KEGG pathway enrichment analysis via GSEA for the (**C**) high and (**D**) low ALOX15 groups. (**E** and **F**) GSVA scores ranking the association of ALOX15 with (**E**) GO terms and (**F**) KEGG pathways.

Immune Infiltration Landscape and Its Correlation with ALOX15

To further investigate the relationship between *ALOX15* and the immune microenvironment, we quantified the infiltration of 22 immune cell types using the CIBERSORT algorithm. The relative proportions of these immune cells showed significant heterogeneity across samples (Figure 8A). Statistical comparison between the healthy and asthma groups (Figure 8B) showed a significant increase in activated mast cells, activated dendritic cells, and neutrophils infiltration in the asthma group. Conversely, M0 and M2 macrophages as well as T follicular helper cells were more abundant in the healthy control group. Furthermore, we performed a correlation analysis to explore the interaction between *ALOX15* and immune cell infiltration. LinkET analysis (Figure 8C) and correlation coefficient plots (Figure 8D) showed that *ALOX15* expression was most strongly positively correlated with eosinophils, resting dendritic cells, and naïve CD4+ T cells. In contrast, *ALOX15* was significantly negatively correlated with activated CD4+ memory T cells, M1/M2 macrophages, and neutrophils. These results suggest that *ALOX15* may play a key role in the regulation of asthma pathogenesis by coordinating the recruitment and activation of specific immune populations, especially eosinophils and mast cells.

https://doi.org/10.2147/JIR.S603984

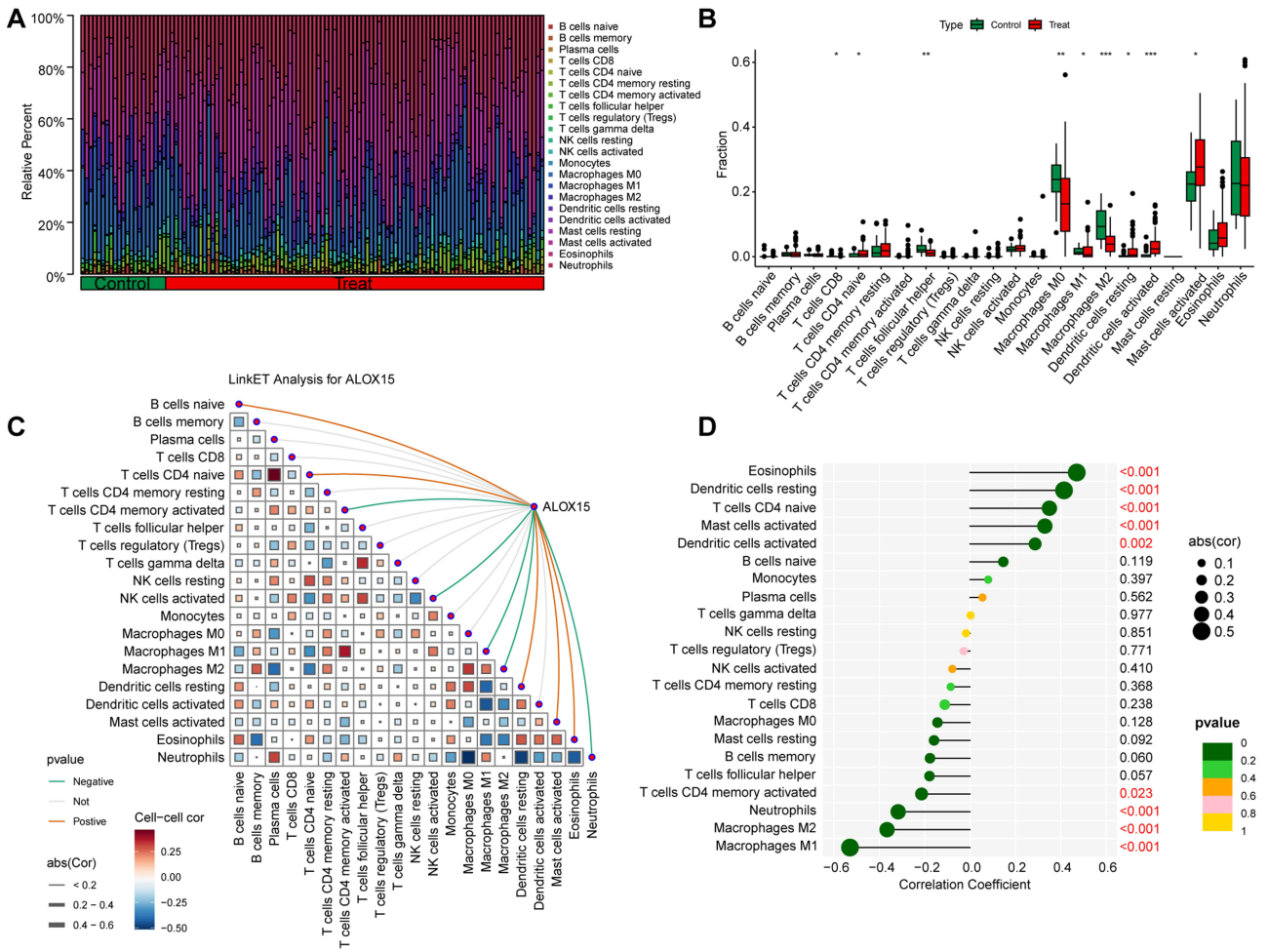

Figure 8 Evaluation of immune cell infiltration and its correlation with ALOX15. (**A**) Stacked bar plot displaying proportions of 22 immune cell types per sample. (**B**) Box plots comparing immune cell abundances between healthy controls and asthma groups. (**C**) LinkET analysis showing the relationship between *ALOX15* expression and the overall immune cell infiltration profile. (**D**) Spearman correlation analysis ranking immune cells based on their correlation coefficients with ALOX15expression. *, $p < 0.05$; **, $p < 0.01$; ***, $p < 0.001$.

Discussion

Obesity significantly increases the prevalence of asthma, yet the molecular mechanisms underlying obesity-induced asthma remain unclear. In this study, we identified and validated ALOX15 as a key molecular bridge linking high-fat diet (HFD)-induced metabolic dysfunction to pro-inflammatory immune responses, thereby driving the onset and exacerbation of asthma in the context of obesity. By combining multi-omic approaches, we established a highly accurate diagnostic framework and localized ALOX15 as a central hub gene for the obesity-associated asthma phenotype. Collectively, our findings highlight ALOX15 as a key molecular bridge between obesity-induced metabolic disorders and airway immune-inflammation, providing new mechanistic insights into obesity-associated asthma.

As a member of the lipoxygenase family, ALOX15 catalyzes the enzymatic oxidation of arachidonic acid to form intermediates that ultimately produce 15-hydroxyeicosatetraenoic acid (15-HETE). These bioactive lipid mediators modulate immune cell migration, airway remodeling, and inflammatory signaling involved in the pathogenesis of several airway diseases.[14] For example, in Lewis lung cancer, ALOX15 has been reported to promote apoptosis and accelerate tumor progression.[16] Previous studies have identified ALOX15 as a biomarker asthma pathogenesis, including ferroptosis of airway epithelial cells and necroptosis-driven inflammation.[17,18] Our study further extends these findings by demonstrating that ALOX15 a key bridging molecule between obesity-related metabolic stress to asthma exacerbation.

Elevated expression of ALOX15 in airway epithelial cells will significantly contribute to inflammation. Type 2 cytokines, including IL-4 and IL-13, activate Jak2/Tyk2 kinases and downstream STAT transcription factors, leading to the upregulation

https://doi.org/10.2147/JIR.S603984

of ALOX15.[14,19] Subsequently, ALOX15 interacts with phosphatidylethanolamine-binding protein 1 (PEBP1), which activates the MEK–ERK signaling cascade and promoting eosinophil-driven airway inflammation.[20] ALOX15-mediated conversion of arachidonic acid to 15-HETE plays a key role in mucus hypersecretion.[21] In vitro studies have shown that IL-13-induced 15-HETE significantly enhances MUC5AC expression in human airway epithelial cells, and elevated ALOX15 activity correlates with increased MUC5AC levels in patients with asthma.[22] Given that MUC5AC expression is tightly associated with asthma severity,[23,24] ALOX15 overexpression may indirectly aggravate disease progression by amplifying mucus overproduction.

In addition to eosinophil-dependent mechanisms, IL-4 and IL-13 have been shown to promote airway remodeling, inflammation, and lung function decline through eosinophil-independent pathways.[25] Consistent with our immune infiltration analysis, ALOX15 expression was positively correlated with eosinophil abundance, supporting its role as a marker of eosinophilic inflammation. Eosinophils are major sources of TGF-β in asthmatic airway. TGF-β drives myofibroblast differentiation and osteopontin transcription, thereby enhancing extracellular matrix deposition and airway remodeling.[26] Notably, our enrichment analyses also revealed significant involvement of the NF-κB signaling pathway in HFD-induced, obesity-related asthma. NF-κB is a master regulator of inflammatory and immune responses, and its pharmacological inhibition has been shown to attenuate LPS-induced lung injury in murine models.[27,28] Clinical evidence also shows that dietary fat promotes oxidative stress and inflammation via Toll-like receptor and ROS-activated NF-κB signaling, thereby contributing to asthma exacerbations.[29]

High-fat diet is a prototypical pro-inflammatory diet linked to chronic inflammatory diseases.[30] Excessive saturated fatty acids activate pattern-recognition receptors and downstream inflammatory cascades.[31] ALOX15-mediated lipid peroxidation further amplifies this inflammatory milieu. Compared with wild-type controls, ALOX15-deficient mice exhibit significantly attenuated inflammatory responses in asthma models.[32] Moreover, elevated ALOX15 expression in human airway epithelial cells disrupts redox homeostasis, enhances type 2 inflammatory signaling, and promotes oxidative stress–induced cell death, thereby exacerbating asthma severity.[18]

Despite the robust validation of ALOX15 through both bioinformatic and experimental approaches, several limitations should be acknowledged. First, the clinical data were derived from public databases with limited longitudinal follow-up, which restricts our ability to assess the long-term prognostic value of ALOX15. Second, although the HFD-induced mouse model effectively mimics human obesity-associated asthma, animal models cannot fully encapsulate the heterogeneity of human patients. Finally, while we identified significant correlations between ALOX15 and immune cell infiltration, the exact molecular mechanisms by which ALOX15 modulates specific immune subsets remain to be fully elucidated through loss-of-function or gain-of-function studies.

In conclusion, this study systematically elucidates the molecular mechanisms underlying the development high-fat diet-induced, obesity-exacerbated asthma from integrated immunological and inflammatory perspectives. By combining bioinformatic analyses with experimental validation, we identify ALOX15 as a central hub gene linking lipid metabolic dysregulation to pro-inflammatory immune responses. These findings suggest that ALOX15 holds promise as a diagnostic biomarker and potential therapeutic target for obesity-associated asthma. However, its clinical applicability and therapeutic value need to be further validated in large-scale patient cohorts and interventional studies.

Declaration of Generative AI and AI-Assisted Technologies in the Writing Process

During the preparation of this work the authors used Gemini in order to improve language only. After using this tool/service, the authors reviewed and edited the content as needed and take full responsibility for the content of the published article.

Data Sharing Statement

All of the datasets used in this study came from publicly accessible resources found at Gene Expression Omnibus (http://www.ncbi.nlm.nih.gov/geo). The experimental data supporting the findings of this study are available from the corresponding author upon reasonable request.

Ethics Approval and Consent to Participate

The animal data involved in this study were approved by the Animal Care and Use Committee of Xiamen Medical College (Approval No. 20250804026) and strictly adhered to the Guide for the Care and Use of Laboratory Animals (8th edition, 2011, National Institutes of Health, USA) and the ARRIVE guidelines. The human data used are publicly available and, in accordance with Article 32 of China's "Measures for Ethical Review of Life Science and Medical Research Involving Humans", are exempt from ethical review.

Author Contributions

Hongsen Zhang: Investigation, Formal analysis, Writing - original draft, Visualization. Linjie Chen, Haojie Chen, Kunyi Zhang, Zinan Chen: Investigation, Validation, Writing - review & editing. Tongsheng Chen: Conceptualization, Methodology, Supervision, Funding acquisition, Writing - review & editing, Project administration. All authors gave final approval of the version to be published; have agreed on the journal to which the article has been submitted; and agree to be accountable for all aspects of the work.

Funding

This work was supported by grants from Guided Healthcare Project of Xiamen, China (3502Z20254ZD1225); Joint Funds for the Innovation of Science and Technology, Fujian Province (2025Y9771); Key Project of 2025 Fujian Provincial Science and Technology Project for Traditional Chinese Medicine (2025ZDB009); Natural Science Foundation of Fujian Province, China (2026J0011844, 2022J05318); Doctoral Start-up Foundation of Xiamen Medical College (K2021-12).

Disclosure

The authors declare no conflict of interest.

References

1. Zhang W, Zhang Y, Li L, Chen R, Shi F. Unraveling heterogeneity and treatment of asthma through integrating multi-omics data. *Front Allergy*. 2024;5:1496392. doi:10.3389/falgy.2024.1496392
2. Bantulà M, Roca-Ferrer J, Arismendi E, Picado C. Asthma and obesity: two diseases on the rise and bridged by inflammation. *J Clin Med*. 2021;10:169. doi:10.3390/jcm10020169
3. Chen L, Chen H, Chen Z, et al. Visceral obesity, partly mediated by a reduction in HDL-C, increases the risk of asthma: insights from NHANES and mendelian randomization studies. *Respir Med*. 2025;249:108482. doi:10.1016/j.rmed.2025.108482
4. Shailesh H, Bhat AA, Janahi IA. Obesity-associated non-T2 mechanisms in obese asthmatic individuals. *Biomedicines*. 2023;11:2797. doi:10.3390/biomedicines11102797
5. Soujanya KV, Jayadeep AP. Obesity-associated biochemical markers of inflammation and the role of grain phytochemicals. *J Food Biochem*. 2022;46:e14257. doi:10.1111/jfbc.14257
6. Bantulà M, Tubita V, Roca-Ferrer J, et al. Differences in inflammatory cytokine profile in obesity-associated asthma: effects of weight loss. *J Clin Med*. 2022;11:3782. doi:10.3390/jcm11133782
7. Specjalski K, Romantowski J, Niedoszytko M. YKL-40 as a possible marker of neutrophilic asthma. *Front Med*. 2023;10:1115938. doi:10.3389/fmed.2023.1115938
8. Rohm TV, Meier DT, Olefsky JM, Donath MY. Inflammation in obesity, diabetes, and related disorders. *Immunity*. 2022;55:31–55. doi:10.1016/j.immuni.2021.12.013
9. Palma G, Sorice GP, Genchi VA, et al. Adipose tissue inflammation and pulmonary dysfunction in obesity. *Int J Mol Sci*. 2022;23:7349. doi:10.3390/ijms23137349
10. Yuan Y, Ran N, Xiong L, et al. Obesity-related asthma: immune regulation and potential targeted therapies. *J Immunol Res*. 2018;2018:1943497. doi:10.1155/2018/1943497
11. Yan J, Horng T. Lipid metabolism in regulation of macrophage functions. *Trends Cell Biol*. 2020;30:979–989. doi:10.1016/j.tcb.2020.09.006
12. Rastogi D, Holguin F. Metabolic dysregulation, systemic inflammation, and pediatric obesity-related asthma. *Ann Am Thorac Soc*. 2017;14:S363–S367. doi:10.1513/AnnalsATS.201703-231AW
13. Schauberger E, Peinhaupt M, Cazares T, Lindsley AW. Lipid mediators of allergic disease: pathways, treatments, and emerging therapeutic targets. *Curr Allergy Asthma Rep*. 2016;16:48. doi:10.1007/s11882-016-0628-3
14. Xu X, Li J, Zhang Y, Zhang L. Arachidonic acid 15-lipoxygenase: effects of its expression, metabolites, and genetic and epigenetic variations on airway inflammation. *Allergy Asthma Immunol Res*. 2021;13:684–696. doi:10.4168/aair.2021.13.5.684
15. Ito E, Hayashizaki R, Hosaka T, et al. Eosinophils and pleural macrophages counter regulate IL-33-elicited airway inflammation via the 12/15-lipoxygenase pathway. *Front Immunol*. 2025;16:1565670. doi:10.3389/fimmu.2025.1565670
16. Sultan M, Ben-Shushan D, Peled M, et al. Specific overexpression of 15-lipoxygenase in endothelial cells promotes cancer cell death in an in vivo lewis lung carcinoma mouse model. *Adv Med Sci*. 2020;65:111–119. doi:10.1016/j.advms.2019.11.006

17. Zhang W, Huang F, Ding X, et al. Identifying ALOX15-initiated lipid peroxidation increases susceptibility to ferroptosis in asthma epithelial cells. *Biochim Biophys Acta BBA - Mol Basis Dis*. 2024;1870:167176. doi:10.1016/j.bbadis.2024.167176
18. Nagasaki T, Schuyler AJ, Zhao J, et al. 15LO1 dictates glutathione redox changes in asthmatic airway epithelium to worsen type 2 inflammation. *J Clin Invest*. 2022;132:e151685. doi:10.1172/JCI151685
19. Bhattacharjee A, Shukla M, Yakubenko VP, et al. IL-4 and IL-13 employ discrete signaling pathways for target gene expression in alternatively activated monocytes/macrophages. *Free Radic Biol Med*. 2013;54:1–16. doi:10.1016/j.freeradbiomed.2012.10.553
20. Zhao J, O'Donnell VB, Balzar S, et al. 15-lipoxygenase 1 interacts with phosphatidylethanolamine-binding protein to regulate MAPK signaling in human airway epithelial cells. *Proc Natl Acad Sci U S A*. 2011;108:14246–14251. doi:10.1073/pnas.1018075108
21. Zhao J, Minami Y, Etling E, et al. Preferential generation of 15-HETE-PE induced by IL-13 regulates goblet cell differentiation in human airway epithelial cells. *Am J Respir Cell Mol Biol*. 2017;57:692–701. doi:10.1165/rcmb.2017-0031OC
22. Zhao J, Maskrey B, Balzar S, et al. Interleukin-13-induced MUC5AC is regulated by 15-lipoxygenase 1 pathway in human bronchial epithelial cells. *Am J Respir Crit Care Med*. 2009;179:782–790. doi:10.1164/rccm.200811-1744OC
23. Altman MC, Flynn K, Rosasco MG, et al. Inducible expression quantitative trait locus analysis of the MUC5AC gene in asthma in urban populations of children. *J Allergy Clin Immunol*. 2021;148:1505–1514. doi:10.1016/j.jaci.2021.04.035
24. Bonser LR, Erle DJ. Airway mucus and asthma: the role of MUC5AC and MUC5B. *J Clin Med*. 2017;6:112. doi:10.3390/jcm6120112
25. Sahnoon L, Bajbouj K, Mahboub B, Hamoudi R, Hamid Q. Targeting IL-13 and IL-4 in asthma: therapeutic implications on airway remodeling in severe asthma. *Clin Rev Allergy Immunol*. 2025;68:44. doi:10.1007/s12016-025-09045-2
26. Siddiqui S, Bachert C, Bjermer L, et al. Eosinophils and tissue remodeling: relevance to airway disease. *J Allergy Clin Immunol*. 2023;152:841–857. doi:10.1016/j.jaci.2023.06.005
27. Chen R, Xie F, Zhao J, Yue B. Suppressed nuclear factor-kappa B alleviates lipopolysaccharide-induced acute lung injury through downregulation of CXCR4 mediated by microRNA-194. *Respir Res*. 2020;21:144. doi:10.1186/s12931-020-01391-3
28. Mussbacher M, Derler M, Basílio J, Schmid JA. NF-κB in monocytes and macrophages - an inflammatory master regulator in multitalented immune cells. *Front Immunol*. 2023;14:1134661. doi:10.3389/fimmu.2023.1134661
29. Wood LG. Diet, obesity, and asthma. *Ann Am Thorac Soc*. 2017;14:S332–S338. doi:10.1513/AnnalsATS.201702-124AW
30. Du W, Zou Z-P, Ye B-C, Zhou Y. Gut microbiota and associated metabolites: key players in high-fat diet-induced chronic diseases. *Gut Microbes*. 2025;17:2494703. doi:10.1080/19490976.2025.2494703
31. Robblee MM, Kim C, Abate J, et al. Saturated fatty acids engage an IRE1α-dependent pathway to activate the NLRP3 inflammasome in myeloid cells. *Cell Rep*. 2016;14(11):2611–2623. doi:10.1016/j.celrep.2016.02.053
32. Hajek AR, Lindley AR, Favoreto S, et al. 12/15-lipoxygenase deficiency protects mice from allergic airways inflammation and increases secretory IgA levels. *J Allergy Clin Immunol*. 2008;122:633–639.e3. doi:10.1016/j.jaci.2008.06.021